Research Square

Preprints are preliminary reports that have not undergone peer review.
They should not be considered conclusive, used to inform clinical practice,
or referenced by the media as validated information.

Cutting Power, Surface Roughness and Sound Pressure in Circular Saw Ripsawing of Radiata Pine Plywood

Alfredo Aguilera

aguilera@uach.cl

Universidad Austral de Chile https://orcid.org/0000-0001-8530-9397

José Luis Barros

Universidad Austral de Chile

Research Article

Keywords: Circular saw, plywood, ripsawing, mean-square sound pressure, cutting power, surface roughness

Posted Date: November 19th, 2026

DOI: https://doi.org/10.21203/rs.3.rs-11623047/v1

License: This work is licensed under a Creative Commons Attribution 4.0 International License.
Read Full License

Cutting Power, Surface Roughness and Sound Pressure in Circular Saw Ripsawing of Radiata Pine Plywood

Alfredo Aguilera [1]*, José Luis Barros [2]

[1]Forest Products Laboratory/Instituto de Bosques y Sociedad. Forest Science and Natural Resources Faculty. Universidad Austral de Chile. Valdivia, Chile, https://orcid.org/0000-0001-8530-9397
[2]Acoustic Institute. Faculty of Engineering. Universidad Austral de Chile. Valdivia, Chile, https://orcid.org/0009-0000-7076-1639

Corresponding author: aguilera@uach.cl

Abstract

Direct measurement of cutting power and surface roughness is often impractical in plywood production. This study evaluated whether mean-square sound pressure could serve as a low-cost indicator of cutting power and roughness in plywood ripsawing. Two circular saw blade configurations (Saw A, 80 teeth; Saw B, 48 teeth) were tested on radiata pine plywood of three thicknesses (12, 15, 18 mm) at three feed speeds (7.5–11.8 m/min), giving 18 conditions with cutting power, roughness (Ra, Rz) and sound pressure recorded. Cutting power was associated with blade configuration, feed speed and panel thickness, with a blade × thickness interaction ($R^2 = 0.98$; leave-one-out $Q^2 = 0.96$, repeating the choice of the interaction within each fold); thickness was confounded with panel, and modulus of elasticity did not explain variation ($p = 0.30$). Roughness did not differ between blades; only panel thickness was significant ($p < 0.03$). Sound pressure discriminated blade configuration ($p < 0.001$) but, pooled across blades, not thickness or feed speed. Its overall correlation with cutting power ($r = 0.89$) reflected separate blade clusters: within Saw A it was strong ($r = 0.81$), whereas within Saw B none was detected ($r = -0.35$; $n = 9$). Sound pressure was not correlated with roughness, overall ($|r| < 0.06$; $n = 18$) or within each blade ($|r| < 0.49$, $p > 0.18$; $n = 9$). An exploratory single-predictor model estimated cutting power moderately within Saw A ($Q^2 = 0.54$) but failed within Saw B ($Q^2 = -2.8$); general use requires validation.

Keywords: Circular saw; plywood; ripsawing; mean-square sound pressure; cutting power; surface roughness

1. Introduction

Circular sawing is one of the most common operations in the wood industry, particularly in the production of plywood panels for furniture, construction, and packaging. In a typical plywood mill, ripsawing—cutting along the grain direction of the face veneers—accounts for a significant portion of total energy consumption and directly influences the quality of the final product. Two performance indicators are especially relevant from both economic and technical perspectives: cutting power and surface roughness. Cutting power determines energy costs, tool wear rates, and machine sizing; even small improvements in cutting efficiency can translate into substantial annual savings in high-volume production. Surface roughness, in turn, affects the need for subsequent sanding or finishing operations; poor surface quality increases production time, generates additional dust, and reduces material yield.

Traditionally, evaluating saw performance requires either direct power measurements using wattmeters or data from frequency inverters—which are not always accessible to operators in real time—or offline surface profiling using contact or optical profilometers, which is time-consuming, labour-intensive, and cannot provide real-time feedback. Given these limitations, there is industrial interest in developing indirect, non-intrusive monitoring methods. Sound pressure (noise) generated during cutting is an attractive candidate because microphones are inexpensive and easy to install, measurements are continuous and can be integrated with machine control systems, and operators already use auditory cues to detect anomalies such as a dull saw or unusual material behaviour. However, the quantitative relationships between sound pressure, cutting mechanics, and resulting surface quality in plywood ripsawing are not well established, and this study contributes to this line of research.

The factors affecting cutting power in wood sawing have been studied extensively, with most research focusing on tool geometry, material properties, and cutting parameters. Regarding tool geometry, the number of teeth, tooth angle, kerf width, and saw blade tension all influence cutting forces and energy consumption. Tool geometry and tool wear are recognized as key determinants of cutting forces, as reviewed by Klamecki [1]. Porankiewicz et al. [2] demonstrated that increasing the number of teeth generally reduces the feed per tooth and may lower cutting forces but also increases friction and heat generation. They further showed that tooth geometry interacts with wood density and moisture content, making it difficult to generalize findings across species and products.

Material properties are widely recognized as dominant factors in solid wood machining. Orlowski et al. [3] applied fracture mechanics to model energetic effects in wood sawing, providing a framework for predicting cutting forces and power that goes beyond classical specific cutting resistance models. Denser and stiffer woods require higher power inputs, a relationship that holds across solid wood species [2, 4]. More recently, Nasir and Cool [5] investigated the effects of wood moisture condition (kiln-dried, green, and frozen) on cutting power and surface quality in circular sawing of hem-fir wood, finding that feed speed had the most significant impact on cutting power across all conditions. Similarly, Chuchała et al. [6] demonstrated that wood provenance and density significantly affect cutting forces in sawing of Scots pine, highlighting the importance of material characterization in machining studies. Cutting parameters have also been investigated: higher feed speeds increase material removal rate and thus power consumption, while feed speed has a more complex, often non-linear effect [4]. Most of these studies, however, were conducted on solid wood rather than plywood, which presents additional complexity due to its layered structure, alternating grain orientation, and adhesive layers. Plywood can cause intermittent cutting forces and tool wear patterns different from those observed in solid wood. Moreover, whether panel stiffness plays the same dominant role in plywood as it does in solid wood has not been systematically tested, which is one of the questions addressed in the present study.

Surface roughness in wood cutting is influenced by tool geometry, feed speed, wood anatomy, and tool sharpness. In circular sawing, the theoretical surface roughness can be estimated from the feed per tooth and saw tooth geometry, but actual roughness is often higher due to vibration, runout, and material heterogeneity [7]. Kminiak et al. [8] studied the effect of tool wear on surface quality in circular sawing of beech wood, finding that the number of teeth (24, 40, and 60) significantly influences the resulting surface roughness (Ra). For plywood, the situation is even more complex because roughness measurements may capture different veneer layers depending on the cut depth, and the adhesive layers can cause localized tear-out. Despite its practical importance, few studies have systematically analysed roughness in plywood ripsawing as a function of blade configuration and panel thickness, and this lack of data hampers the optimization of cutting parameters for both quality and efficiency. In addition, whether the effect of tooth count reported for solid wood is reproduced in plywood remains an open question.

Sound pressure and acoustic emission (AE) have been explored in several wood machining contexts as potential monitoring tools. For instance, in a routing study, Iskra and Tanaka [9] found a linear relationship between feed rate and sound intensity, as well as a strong correlation between sound intensity and surface roughness. Cyra and Tanaka [10] demonstrated correlations between AE count rate and surface roughness in routing, establishing that acoustic emission shows promise for monitoring surface quality during wood machining. Extending this line of research, Iskra and Tanaka [11] compared selected acoustic signal analysis techniques to evaluate wood surface roughness produced during routing, further confirming the potential of AE for real-time surface quality assessment. Nasir et al. [12] applied artificial intelligence to acoustic emission monitoring in sawing, showing its potential for optimal sensory feature selection. In a multi-sensor approach, Nasir et al. [13] fused measurements of cutting power, sound, vibration, and acoustic emission to predict tool temperature during circular sawing, reporting that acoustic emission signals provided the best monitoring performance. Chen et al. [14] recently reviewed tool condition monitoring strategies from metal cutting and discussed their applicability to wood-based material processing, highlighting the potential for technology transfer between these manufacturing sectors. In previous work, Aguilera and Martin [15] related cutting forces, power, and roughness in solid wood, and Aguilera and Barros [16] showed that acoustic signals can be related to surface roughness in MDF ripsawing; the present study extends this line of research to plywood. However, those studies focused on solid wood and MDF, which are comparatively homogeneous materials, whereas plywood presents additional complexity due to its layered structure. Despite these findings, the potential of mean-square sound pressure as a process-monitoring variable in plywood ripsawing remains little explored, and its relationship with cutting power and surface roughness under different cutting conditions requires further research.

It is important to distinguish sound pressure from acoustic emission (AE), as both have been used in wood machining monitoring but differ fundamentally in their physical nature and measurement. AE refers to transient elastic waves generated within the material due to the rapid release of stored strain energy from irreversible microstructural changes, such as plastic deformation, crack propagation, and friction at the tool–workpiece interface [17]. These waves typically occupy a frequency range from a few kHz to several hundred kHz and are acquired using piezoelectric transducers mounted in contact with the workpiece or machine structure [17]. In contrast, sound pressure refers to pressure fluctuations propagating through the air, typically within the 20 Hz–20 kHz audible range and is measured with a microphone in a free-field configuration without contact with the workpiece or machine [17]. While AE offers higher sensitivity to localized damage events and a frequency range well above machine vibrations and environmental noise, it requires direct sensor contact, careful surface preparation, and more complex signal processing, and its signals are strongly attenuated in viscoelastic and porous materials such as wood [17]. Sound pressure, although less sensitive to high-frequency damage mechanisms, offers a simpler, non-intrusive, and low-cost alternative that can be easily integrated into industrial environments. This study focuses on sound pressure because the objective is to explore a low-cost monitoring approach that does not require contact sensors or modifications to the cutting tool or workpiece.

The general objective of this study is to evaluate the relationships between sound pressure, cutting power, and surface roughness in plywood ripsawing with circular saws of different blade configurations. The specific objectives are: a) to quantify the effects of blade configuration (Saw A vs. Saw B), panel thickness (12, 15, and 18 mm), and feed speed (7.5, 9.7, and 11.8 m/min) on cutting power, surface roughness (Ra and Rz), and sound pressure, b) to determine whether differences in cutting power between blade configurations persist after accounting for panel stiffness (MOE); c) to establish quantitative correlations between sound pressure and cutting power, and to explore, through

cross-validation, the feasibility of estimating cutting power from sound pressure; and d) to evaluate whether sound pressure is correlated with surface roughness (Ra and Rz).

2. Materials and Methods

Experiments were carried out on radiata pine (*Pinus radiata*) plywood panels with nominal thicknesses of 12, 15 and 18 mm. Each specimen measured 1200 mm in length by 80 mm in width. Prior to testing, all panels were conditioned in a climate chamber at 20°C and 65% relative humidity for one week. The material was characterized by an average moisture content of 8.9% (range 8.5–9.5%, determined by oven-drying method) and an average density of 0.494 g/cm³. These properties were measured solely for material characterization and were not included as explanatory variables in the statistical models.

Two circular saw blades with carbide-tipped alternate top bevel teeth were used. Both blades had a diameter of 250 mm and were designed for cutting wood-based materials. The machining tests were performed with sharp circular saw blades to eliminate tool wear as a variable. Their main linear and geometric characteristics are summarised in Table 1. The blades differ in tooth count (Saw A, 80 teeth; Saw B, 48 teeth; Fig. 1), which also entails differences in tooth pitch, rake angle, and tooth height. Saw A has a smaller rake angle (9° compared to 18°), which in theory increases cutting resistance but may improve surface finish, while Saw B has a larger rake angle, making cutting easier by reducing cutting forces. Additionally, Saw B has a larger tooth pitch and greater tooth height, meaning fewer teeth are in contact with the material at any given time.

Since the two blades differ in several geometric parameters (tooth count, rake angle, tool angle, clearance angle, tooth pitch, and tooth height), all comparisons between them should be interpreted as differences between two blade configurations, not as isolated effects of tooth count. This distinction is maintained throughout the manuscript when referring to the tested tools.

Table 1 Linear, geometrical, and operational parameters of the circular saw blades.

Parameter	Saw blade A	Saw blade B	Operational	Value
Number of teeth	80	48	Spindle speed (rpm)	4048
Cutting diameter (mm)	250	250	Cutting speed (m/s)	53
Rake angle (°)	9	18	Feed speed (m/min)	7.5 – 9.7 – 11.8
Tool angle (°)	70	56	Override (mm)	12
Clearance angle (°)	11	16	Cutting depth (mm)	12 – 15 – 18
Tooth pitch (mm)	9.8	16.4		
Tooth height (mm)	8	11		
Kerf (mm)	3.2	3.2		



Fig. 1 Circular saws used in the experiment: Saw A with 80 teeth (left), saw B with 48 teeth (right).

Tests were performed on a single-spindle machine adapted for circular sawing, with a frequency drive controlling cutting speed and feed. The machining conditions included conventional cutting mode, a constant cutting depth (equal to panel thickness), three levels of feed speed, one level of cutting speed and a constant override of 12 mm (Table 1). The override was carefully adjusted before each test series to remain constant regardless of panel thickness, ensuring that all teeth actively participate in cutting across the entire panel height while avoiding excessive stresses on the blade periphery.

The final experimental matrix consisted of 18 distinct cutting conditions (Table 2), each tested with three successive cuts on the same specimen, resulting in a total of 54 individual cuts (Fig. 2). This design allows the evaluation of main effects across all feed speeds and both blade configurations.

Specimens were obtained from three commercial-sized radiata pine plywood panels, one for each nominal thickness (12, 15 and 18 mm), and cut into samples of the required dimensions. After conditioning, samples from each panel were stored without any predefined order and were randomly assigned to the six combinations of blade configuration and feed speed. This random assignment distributes pre-existing variability in material properties (e.g., density, MOE, veneer quality) randomly across blade configurations and feed speeds within each panel. Because each thickness corresponds to a different panel, thickness and panel are confounded in the design. The experimental unit was the cutting condition (n = 18), defined as a unique combination of panel thickness (12, 15, 18 mm), blade configuration (Saw A or Saw B), and feed speed (7.5, 9.7, 11.8 m/min). The order in which the 18 conditions were tested was randomized. Within each condition, three successive cuts were made consecutively on the same specimen; these cuts are repeated measurements, not independent experimental units, and their values were averaged per condition before statistical analysis to avoid pseudo-replication.

Table 2 Experimental design showing the different cutting setups.

Panel thickness h_c (mm)	Blade configuration	Feed speed v_f (m/min)	Mean chip thickness h_m (mm)
12	A (80 teeth)	7.5	0.0118
12	B (48 teeth)	7.5	0.0197
12	A	9.7	0.0153
12	B	9.7	0.0255
12	A	11.8	0.0186
12	B	11.8	0.0310
15	A	7.5	0.0122
15	B	7.5	0.0204
15	A	9.7	0.0158
15	B	9.7	0.0263
15	A	11.8	0.0192
15	B	11.8	0.0320
18	A	7.5	0.0126
18	B	7.5	0.0210
18	A	9.7	0.0163
18	B	9.7	0.0271
18	A	11.8	0.0198
18	B	11.8	0.0330

Note: Each condition was tested with three successive cuts on the same specimen; values reported are the mean of the three replicates. Roughness values are the mean of six measurements (two strips × three points). All statistical analyses used the condition means (n = 18).

The mean chip thickness (h_m) for each condition was calculated using the formula (1) proposed by [18]:

$$h_m = \frac{1000 \cdot v_f}{n \cdot z \cdot D}\left[\sqrt{(D - h_c - O) \cdot O} + \sqrt{(D - O)(h_c + O)}\right] \quad (1)$$

where v_f is feed speed (m/min), n is rotation speed (4048 rpm), z is the number of teeth, D is saw diameter (250 mm), h_c is panel thickness (mm), and O is override (12 mm).



Fig. 2 Plywood sample after cutting test; three slices were produced for each cutting condition.

After each machining test, every remaining specimen was sectioned (two pieces per specimen) according to UNE-EN 310 standards for modulus of elasticity (MOE) testing. Specimen dimensions were 50 mm in width, with a length equal to 20 times the nominal thickness plus 50 mm; the span between supports was adjusted to exactly 20 times the thickness. MOE was calculated from the load-deflection curve obtained in three-point bending. MOE was not initially considered a controlled

experimental factor because the experimental design focused on blade configuration, panel thickness, and feed speed, which are the parameters typically available to operators in production. MOE was measured post hoc to test whether panel stiffness explained the observed variation in cutting power (see Section 3.1). The MOE of each condition was the mean of the pieces obtained from the specimen of that condition. Future studies interested in the role of panel stiffness should measure MOE before the cutting tests and use it as a blocking factor or covariate in the design.

Power consumption was acquired directly from frequency drive controller (Danfoss VLT Micro Drive FC51) connected to computer, where nine data points per second were recorded during each cut. For each replicate, total power (P_t, kW) was recorded continuously over the period of full blade engagement of the cut. Idle power (P_{idle}, kW) was recorded before and after each test, and net cutting power (P_c, kW) was then obtained by subtraction. The three replicate values were averaged to obtain the condition mean. Fig. 3 shows an example for Saw B at 12 mm panel thickness and 9.7 m/min feed speed.

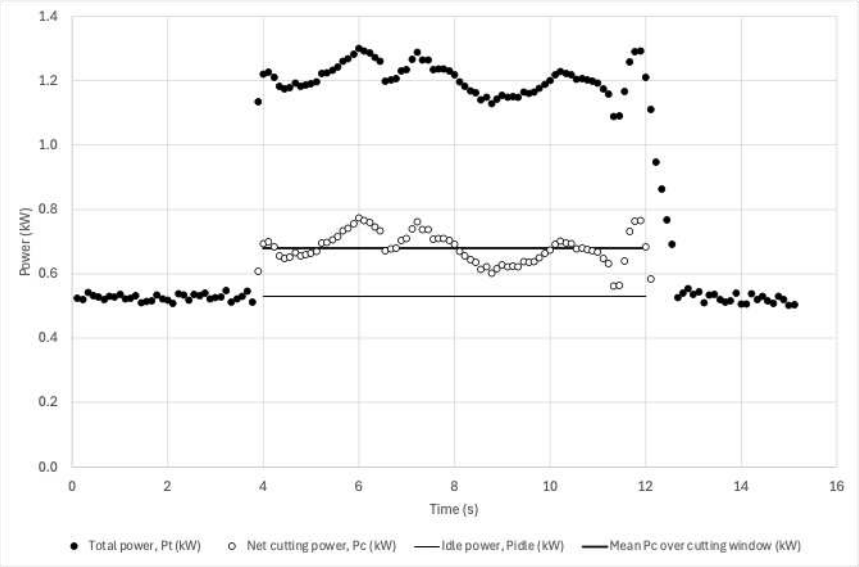


Fig. 3 Example of the power signal recorded during one cut (Saw B, 12 mm, 9.7 m/min). Closed circles: total power (P_t); open circles: net power ($P_t - P_{idle}$). Thin line: mean idle power (P_{idle}); thick line: mean net cutting power (P_c) over the analysis window (4–12 s).

Surface roughness was measured using a contact profilometer (Mitutoyo Surftest SJ-210) following ISO 4287. As reviewed by Gurău and Irle [19], Ra and Rz are the most established parameters for assessing surface quality of wood products. The measurement parameters were cut-off length of 2.5 mm, five sampling lengths, an evaluation length of 12.5 mm, and a standard Gaussian filter. For each cutting condition, two strips were obtained, and roughness was measured at three points per strip along the feed direction, approximately in the middle section of each strip. The average of these six measurements was used as the roughness value for each condition. Arithmetic mean roughness (Ra, µm) and mean peak-to-valley height (Rz, µm) were recorded for each specimen. Both parameters were measured because they capture complementary aspects of surface topography. Ra represents the average deviation of the roughness profile from the mean line and is the most commonly reported roughness parameter in wood machining studies [20]. However, Ra is insensitive to isolated peaks or valleys, which can be critical for plywood due to localized tear-out of veneer layers. Rz, which measures the average distance between the highest peak and deepest valley over five sampling lengths, provides additional information about extreme surface irregularities that may affect

subsequent finishing operations such as sanding or coating. Other parameters were not considered because they offer limited additional information for the purpose of this study and are less commonly reported in the wood cutting literature.

Sound pressure was recorded using a free-field measurement microphone (Earthworks M30 BX) placed 40 cm from the cutting zone, at an approximate 45° angle to the feed direction. This position was selected to avoid directional effects and to capture the overall sound radiated from the cutting process without saturating the microphone. The microphone was connected to a high-fidelity digital recorder (Sound Devices 888), and signals were acquired at a sampling rate of 48 kHz.

Prior to each measurement session, the microphone was calibrated using a pistonphone. Calibration was verified at the beginning and end of each session; no drift exceeding ±0.5 dB was observed across sessions. The recorded signals were processed offline to obtain the root mean square (RMS) sound pressure. RMS sound pressure was selected as the primary acoustic feature because it provides a simple, robust, and computationally efficient measure of the overall acoustic pressure fluctuations generated during cutting. The reported values correspond to the mean-square sound pressure, calculated as the square of the RMS pressure and expressed in Pa^2. Under appropriate acoustic field conditions, this quantity is proportional to sound intensity in a given medium; however, it is not a direct measurement of acoustic intensity or acoustic power. While frequency-domain features such as spectral peaks or tooth-pass frequency components ($n \times z / 60$) could provide additional diagnostic information, they require more complex signal processing and prior knowledge of the blade configuration, which may not be available in industrial settings. The RMS approach is therefore potentially more suitable for a low-cost, real-time monitoring system.

Preliminary tests were conducted to verify microphone placement and recording levels. The background noise level (including all possible noise sources before the cut) was measured at 85 dB sound pressure level (SPL), which corresponds to a mean square sound pressure of approximately 0.126 Pa^2. During cutting, the sound pressure level was at least 103 dB SPL in every cut (lowest individual cut: 8.8 Pa^2, 103.4 dB SPL; lowest condition mean: 14.8 Pa^2, 105.7 dB SPL). The cutting signal therefore exceeded the background level by at least 18 dB (a factor of about 70 in Pa^2), above the commonly recommended signal-to-noise margin of 10 dB, so background contributions were negligible. The conversion from mean square sound pressure (Pa^2) to sound pressure level (dB SPL) follows the standard formula: $SPL = 10 \log_{10} (p^2_{rms}/p^2_0)$ with $p_0 = 20$ μPa as the reference pressure.

Statistical analyses were performed using Python with the statsmodels library. Descriptive statistics (mean, standard deviation, minimum, maximum) were calculated for each experimental condition. Pearson correlation was used to assess linear relationships among continuous variables, including those between mean-square sound pressure and each roughness parameter (Ra, Rz), computed using the 18 condition means and, separately, within each blade configuration ($n = 9$). Spearman rank correlations were also calculated to check robustness to non-linearity. Multiple linear regression with ordinary least squares was applied for each response variable. Analysis of variance (ANOVA) and covariance (ANCOVA) were used to determine the significance of main effects and interactions, with MOE included as a covariate where indicated. The significance level was set at $\alpha = 0.05$ for all tests. All regression and ANCOVA models were fitted using the condition means ($n = 18$). In models including interaction terms, continuous predictors were centred at the mean of the design and blade configuration was coded −0.5/+0.5, so that main-effect coefficients and their partial η^2 (Type III) refer to average effects within the experimental range; the equivalent model in natural units is also reported (Eq. 2).

The predictors of Eq. 2 were the three design factors (blade configuration, panel thickness, and feed speed) and the saw × thickness interaction, which was retained because the residuals of the additive

model showed a curved pattern (Section 3.1); no further variable selection was applied to Eq. 2. MOE was evaluated as an additional covariate to determine whether panel stiffness explained variation in cutting power beyond the effects of the experimental design factors. Density and moisture content were used only to characterize the plywood material and were not included in the statistical models. Because mean-square sound pressure was strongly associated with blade configuration (the two configurations formed distinct acoustic clusters), their joint inclusion was evaluated by comparing cross-validated predictive performance rather than by interpreting individual coefficients.

Predictive performance was assessed by leave-one-out cross-validation (LOOCV): each of the 18 observations was left out in turn, the model was re-fitted to the remaining 17, and the left-out observation was predicted. From the 18 out-of-fold predictions, $Q^2 = 1 - \text{PRESS/TSS}$ (PRESS: sum of squared prediction errors; TSS: total sum of squares about the mean; $Q^2 < 0$ indicates predictions worse than the mean), RMSECV and MAECV (root mean square and mean absolute prediction errors) were computed. Because the saw × thickness interaction was introduced after inspecting the residuals, the model selection was repeated within each training set (nested LOOCV): the model with the lowest corrected Akaike information criterion (AICc) among the additive model and five alternatives (adding saw × thickness, saw × feed speed, thickness × feed speed, quadratic thickness, or saw × thickness plus quadratic thickness) was selected and used to predict the left-out observation.

Normality of residuals was checked with the Shapiro–Wilk test, homoscedasticity with the Breusch–Pagan test, multicollinearity with the variance inflation factor (VIF), and influence with Cook's D. When heteroscedasticity was detected, robust standard errors (HC3) were used.

To explore the feasibility of estimating cutting power from sound pressure, a simplified model was fitted with cutting power as the response variable and sound pressure as the predictor, because ordinary least-squares regression is directional and algebraic rearrangement of a model fitted in the opposite direction is not statistically valid. Blade configuration was also tested as an additional predictor, and the choice was based on LOOCV performance (Section 3.3).

3. Results and Discussion

3.1 Cutting power

Fig. 4 presents the cutting power as a function of panel thickness for both saws (averaged over the three feed speeds). Raw values suggest that Saw B (48 teeth) consumes less power than Saw A (80 teeth) across all thicknesses. Cutting power for Saw A increases with panel thickness, from 1.43 kW at 12 mm to 2.16 kW at 18 mm (+51%). For Saw B, the increase is smaller: from 0.69 kW to 0.96 kW (+39%).

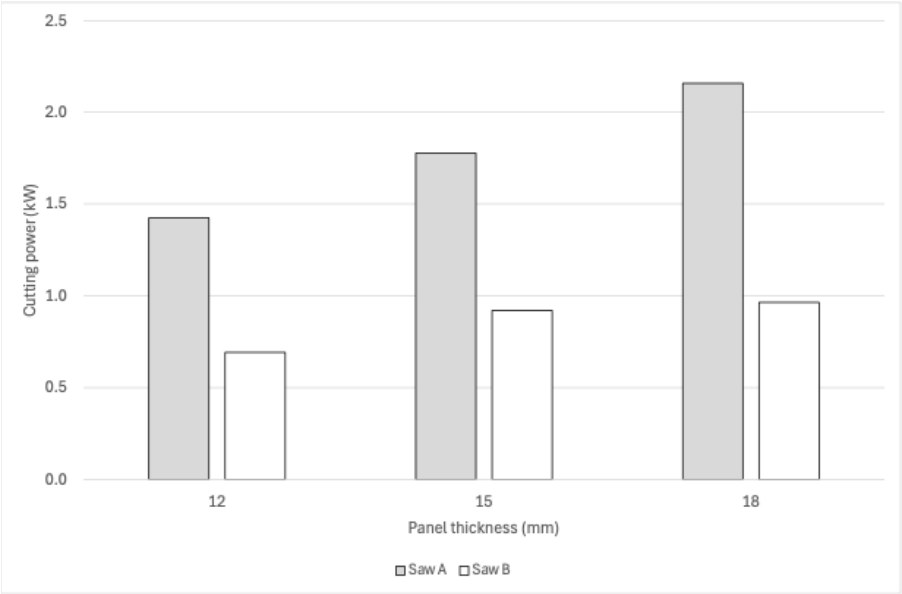


Fig. 4 Cutting power as a function of panel thickness for both saws.

An ANCOVA with cutting power as the response, blade configuration as a factor, and MOE as a covariate showed that MOE did not explain cutting power ($F = 1.14$, $p = 0.30$), whereas blade configuration was highly significant ($F = 56.0$, $p < 0.001$). This contrasts with the strong MOE–power relationship reported for solid wood [2, 4] and suggests that, within the range evaluated in this study, panel stiffness did not significantly explain the observed variation in cutting power for plywood. In a simple regression on MOE alone, $R^2 = 0.01$ ($p = 0.70$; Fig. 5). Mean MOE values by panel thickness and blade configuration are summarized in Table 3.

Table 3. Mean MOE values (GPa) by panel thickness and blade configuration.

Panel thickness h_c (mm)	Saw A (80 teeth)	Saw B (48 teeth)
12	4.25	3.86
15	4.20	4.47
18	4.31	4.56
Overall mean	4.25	4.30

Note: MOE values are means of the condition means (n = 18) for each panel thickness and blade configuration (three feed speeds each). Individual MOE measurements ranged from 3.24 to 6.69 GPa; the range of condition means is 3.58–6.21 GPa.

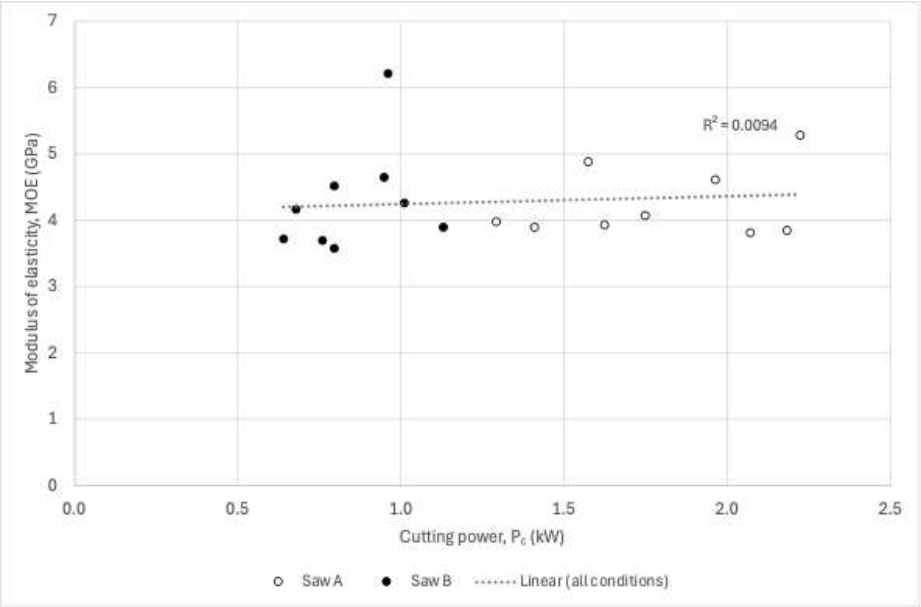


Fig. 5 Cutting power (P_c) versus modulus of elasticity (MOE) for the 18 experimental conditions. Open circles: Saw A; filled circles: Saw B. Dotted line: global linear fit ($R^2 = 0.0094$).

A multiple regression model with blade configuration, panel thickness, and feed speed as predictors explained 94.8% of the variance in cutting power ($R^2 = 0.948$; LOOCV $Q^2 = 0.91$; RMSECV = 0.16 kW), but its residuals showed a curved pattern against the fitted values (quadratic term, $p = 0.005$), reflecting the significant saw × thickness interaction. A model including this interaction ($n = 18$) was therefore adopted. Because the interaction term was introduced after inspecting the residuals of the additive model, the model selection was repeated within each training set (nested LOOCV, see Methods): the saw × thickness interaction was selected in all 18 folds, and the nested Q^2 (0.96; RMSECV = 0.11 kW) was essentially identical to the non-nested value. Residual diagnostics for Eq. 2 are discussed in Section 3.3.

$$P_c = -0.486 + 0.231 \cdot I_B + 0.122 \cdot h_c - 0.077 \cdot I_B \cdot h_c + 0.046 \cdot v_f \quad (2)$$

where P_c is in kW, $I_B = 1$ for Saw B (48 teeth) and 0 for Saw A (80 teeth), h_c is panel thickness in mm, and v_f is feed speed in m/min. The model achieved $R^2 = 0.98$ (adjusted $R^2 = 0.97$), and all effects in Table 4 were significant ($p \leq 0.002$). The thickness slope was 0.122 kW/mm for Saw A and 0.045 kW/mm for Saw B. Because the coefficients of Eq. 2 refer to zero thickness and zero feed speed (outside the tested range), Table 4 reports the same model with centred predictors, together with 95% confidence intervals and partial effect sizes.

Blade configuration had a very large effect (partial $\eta^2 = 0.97$), followed by panel thickness (0.88), the saw × thickness interaction (0.62), and feed speed (0.54). Saw B consumed less power than Saw A by 0.70 kW at 12 mm (95% CI −0.84 to −0.56), 0.93 kW at 15 mm (−1.02 to −0.84), and 1.16 kW at 18 mm (−1.30 to −1.02).

Table 4. Multiple regression of cutting power (kW) on blade configuration, panel thickness, feed speed, and the saw × thickness interaction (centred model, equivalent to Eq. 2).

Effect	Coefficient	95% CI	p	Partial η^2	Same term in Eq. 2
Intercept (mean of both saws at 15 mm and 9.67 m/min)	1.323	1.279, 1.368	<0.001	—	-0.486
Blade configuration (Saw B – Saw A, at 15 mm)	-0.930	-1.019, -0.841	<0.001	0.97	0.231
Panel thickness (mean slope of both saws, per mm)	0.084	0.065, 0.102	<0.001	0.88	0.122
Feed speed (per m/min)	0.046	0.020, 0.071	0.002	0.54	0.046
Saw × thickness interaction	-0.077	-0.114, -0.041	<0.001	0.62	-0.077

Note: n = 18 condition means. Predictors were centred so that main-effect coefficients are interpretable in the presence of the saw × thickness interaction: panel thickness at 15 mm, feed speed at 9.67 m/min, and blade configuration coded −0.5 (Saw A) and +0.5 (Saw B). Consequently, the blade coefficient is the Saw B − Saw A difference at 15 mm, the thickness coefficient is the mean slope of the two saws, and the intercept is the mean cutting power of both saws at 15 mm and 9.67 m/min. This is the same model as Eq. 2 ($R^2 = 0.98$; identical fitted values and residuals). The last column gives the coefficients of Eq. 2, which refer to zero thickness and zero feed speed (outside the experimental range) and cannot be interpreted separately; they are related to the centred coefficients by: blade = 0.231 − 0.077 × 15 = −0.930; thickness = 0.122 − 0.077/2 = 0.084 (computed from unrounded coefficients; with the rounded values shown, the results are −0.924 and 0.0835). Partial η^2 from Type III sums of squares. CIs based on OLS standard errors (Breusch–Pagan p = 0.06).

Saw B reduced cutting power relative to Saw A within every panel (Table 4). Because each thickness corresponds to a different panel (Section 2), the thickness effect and the saw × thickness interaction cannot be separated from panel-to-panel differences (e.g., density, veneer quality, adhesive), and the thickness coefficients in Eq. 2 and Table 4 describe the three panels tested rather than a general effect of thickness. Since cutting depth equals panel thickness, an increase of power with thickness is mechanically expected, but its magnitude, and the apparent increase of the blade difference with thickness, should be regarded as specific to these panels. In contrast, the Saw B − Saw A difference within each panel is not affected by this confounding, because specimens were randomly assigned to blade configuration and feed speed. This difference is attributable to the combined effect of the geometric parameters that define each blade configuration (tooth count, rake angle, tooth pitch, and tooth height), not to tooth count alone.

3.2 Surface roughness

Surface roughness values (Ra) ranged from 2.01 to 6.93 µm across individual measurements, and from 3.19 to 5.56 µm when averaged by condition (Fig. 6). The lowest condition-mean Ra was obtained with Saw A at 15 mm (3.19 µm at 7.5 m/min), while Saw B condition means ranged from 3.59 to 5.56 µm.

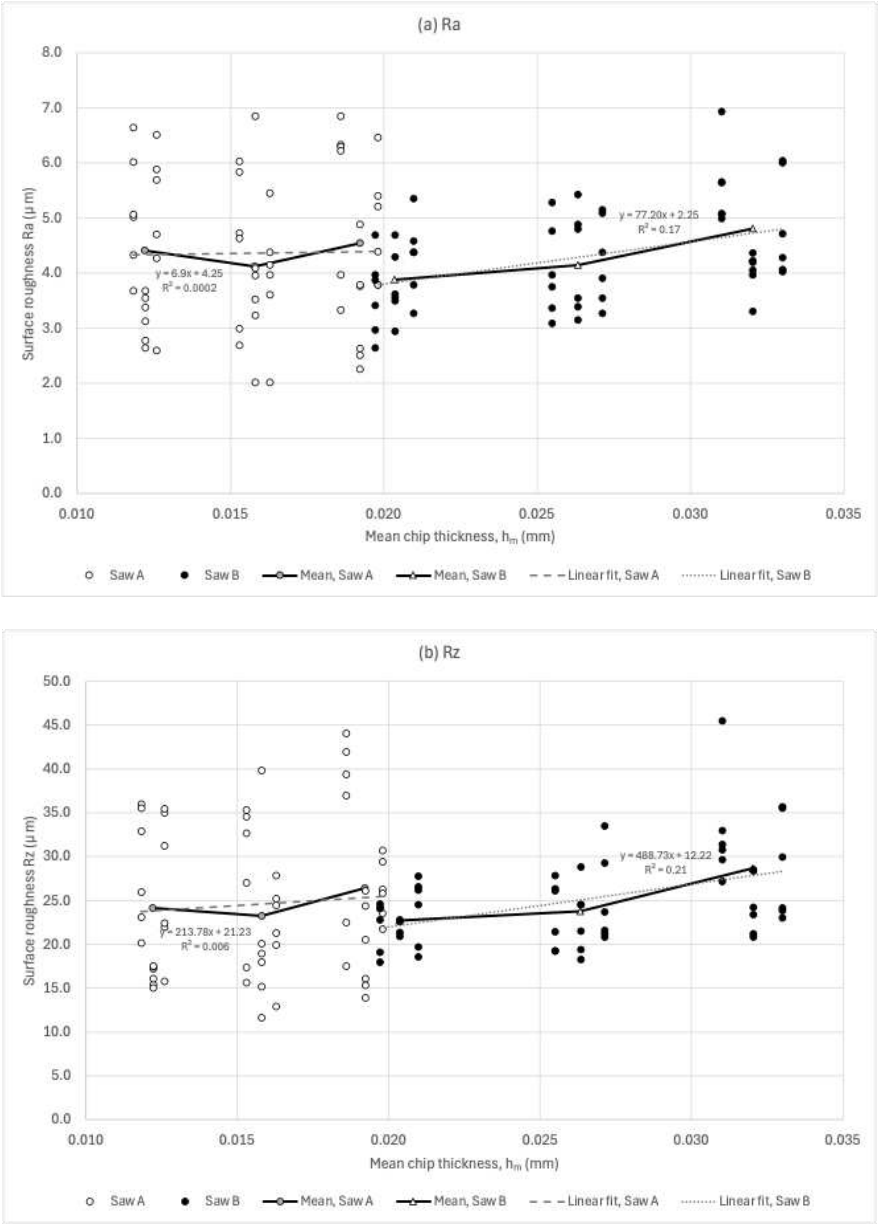


Fig. 6 Surface roughness Ra (a) and Rz (b) as a function of mean chip thickness (h_m). Open circles: Saw A; filled circles: Saw B (individual measurements; two strips × three points per condition). Solid lines connect the means of the conditions sharing the same feed speed for each saw (n = 3 per point); dashed (Saw A) and dotted (Saw B) lines are linear fits to the individual measurements, with their R^2 (individual measurements, not condition means; shown for illustration only, as statistical inference is based on condition means).

The difference between saws was negligible when averaged over all conditions: mean Ra was 4.36 µm for Saw A and 4.28 µm for Saw B. The coefficients of variation for Ra ranged from 9% to 41% across conditions, with the highest variability for Saw A at 15 mm (up to 41%), while the CVs of the Saw B conditions did not exceed 23%.

Multiple regression analysis (n = 18) supported this interpretation. With blade configuration, panel thickness (as a continuous variable), and feed speed as predictors, no term was significant for Ra or Rz (R^2 = 0.12 and 0.21, respectively), and using mean chip thickness instead of thickness and feed speed did not change this result (in models with blade configuration and h_m, the p-values for h_m were 0.18 for Ra and 0.13 for Rz). Panel thickness reached significance only when treated as a three-level factor in a three-factor ANOVA (Ra p = 0.026; Rz p = 0.006; Table 5), whereas blade configuration was not significant (p = 0.77 for Ra and 0.76 for Rz) and feed speed was not significant for Ra (p = 0.20) and marginal for Rz (p = 0.061). The differences among thickness levels were not monotonic (Ra = 4.71, 3.73, and 4.51 µm; Rz = 28.0, 21.0, and 25.5 µm for 12, 15, and 18 mm), which points to panel-to-panel variability rather than a thickness effect. Roughness is therefore dominated by local factors not captured by the measured variables, such as veneer tear-out, adhesive layer behaviour, and density gradients.

Table 5. ANOVA results for Ra and Rz (three-factor model: blade configuration, panel thickness, feed speed).

Response	**Factor**	**F**	**p**
Ra	Blade configuration	0.09	0.77
Ra	Panel thickness	5.06	0.026
Ra	Feed speed	1.82	0.20
Rz	Blade configuration	0.10	0.76
Rz	Panel thickness	7.99	0.006
Rz	Feed speed	3.55	0.061

Note: Degrees of freedom: 1,12 (blade configuration); 2,12 (panel thickness and feed speed). Main-effects fitted to condition means (n = 18).

Within each blade configuration (Fig. 6), Ra and Rz did not vary with mean chip thickness for Saw A ($R^2 \leq 0.02$, $p > 0.7$, n = 9 condition means). For Saw B, both parameters tended to increase with h_m (Ra: 77 µm/mm, R^2 = 0.43, p = 0.053; Rz: 489 µm/mm, R^2 = 0.49, p = 0.035; n = 9 condition means), as expected from the kinematics of chip formation [21]. This relationship is exploratory given the small sample, and because h_m is determined jointly by panel thickness and feed speed. The R^2 values shown in Fig. 6 were calculated from individual measurements (n = 54 per blade configuration) and are therefore lower than those obtained from condition means.

These results show no advantage of either blade configuration in surface finish. Mean Rz (24.6 vs. 25.0 µm) was practically identical between saws, and the high within-condition variability means that any apparent difference in individual conditions is not statistically meaningful. The practical

implication is that, for radiata pine plywood ripsawing with sharp blades, blade configuration is not a lever for improving surface quality within the range tested; differences among panels (confounded with thickness) and local veneer quality are more influential. Future studies should consider complementary roughness parameters (e.g., Rk or 3D surface descriptors) and should measure veneer quality before cutting to better capture the sources of variability.

3.3 Sound pressure and cutting power

Mean-square sound pressure was consistently higher for Saw A (27.8–44.2 Pa^2) than for Saw B (14.8–25.3 Pa^2), with no overlap between the two groups. In a three-factor ANOVA of main effects, it depended strongly on blade configuration ($F(1,12) = 57.2$, $p < 0.001$) but not on panel thickness ($p = 0.63$) or feed speed ($p = 0.48$); within Saw A, however, it increased with panel thickness ($p = 0.013$, adjusted for feed speed, $n = 9$).

Fig. 7 shows mean-square sound pressure (p^2_{rms}, Pa^2) plotted against cutting power (P_c). The overall correlation is strong ($r = 0.89$), but the plot reveals two clearly separated clusters, and the two blade configurations do not overlap on either axis (Saw A: 1.29–2.22 kW; Saw B: 0.64–1.13 kW). When the correlation is computed within each configuration, the picture changes: within Saw A, $r = 0.81$ ($R^2 = 0.66$, $p = 0.008$), whereas within Saw B, $r = -0.35$ ($R^2 = 0.12$, $p = 0.36$), i.e., no detectable relationship. The overall correlation therefore reflects, to a large extent, the difference between configurations rather than a relationship that holds universally between mean-square sound pressure and cutting power.

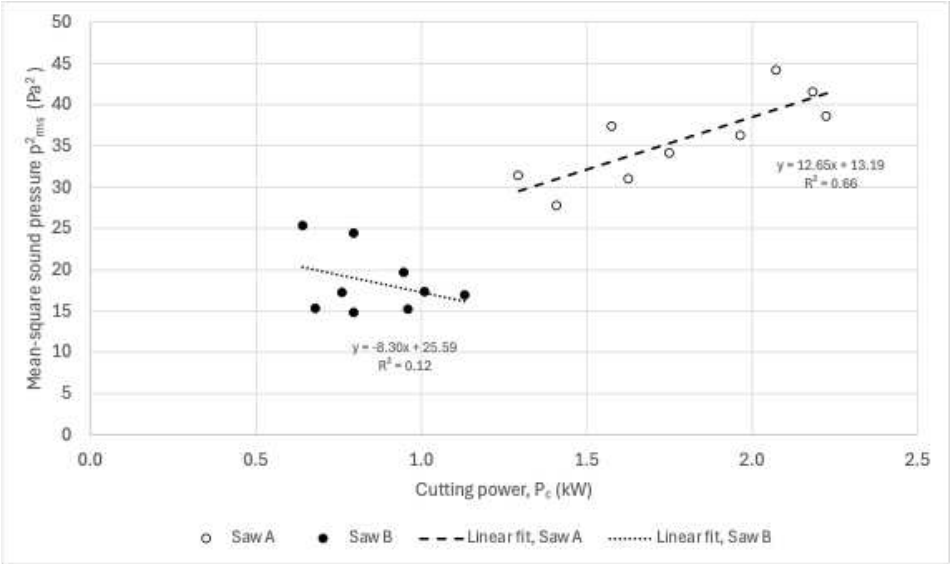


Fig. 7 Mean-square sound pressure (p^2_{rms}, Pa^2) versus cutting power (P_c) for the 18 experimental conditions. Open circles: Saw A; filled circles: Saw B. Dashed (Saw A) and dotted (Saw B) lines: linear fits for each configuration.

Consistent with this, a regression with mean-square sound pressure as the response and cutting power, blade configuration, and MOE as predictors explained 85% of the variance in p^2_{rms} ($R^2 = 0.85$). Cutting power was significant ($p = 0.040$), blade configuration was marginal ($p = 0.069$), and MOE was not significant ($p = 0.55$). Given the limited sample size ($n = 18$) and the strong association between P_c and blade configuration, individual coefficients in this model should not be over-interpreted.

From a monitoring perspective, the relevant question is the reverse: can cutting power be estimated from mean-square sound pressure? A model fitted in the prediction direction, with P_c as the response and p^2_{rms} as the only predictor, achieved $R^2 = 0.80$ and a leave-one-out cross-validated $Q^2 = 0.75$. Previous research has investigated the relationship between sound intensity and power consumption in wood machining [22, 23]. Based on the present experimental data, the following regression equation was obtained to estimate cutting power from mean-square sound pressure:

$$P_c = 0.0065 + 0.0485 \cdot p^2_{rms} \quad (3)$$

where P_c is expressed in kW and p^2_{rms} represents the mean-square sound pressure, expressed in Pa^2. The cross-validated RMSE was 0.26 kW and the cross-validated MAE was 0.21 kW (Fig. 8). Adding blade configuration did not improve out-of-sample performance ($Q^2 = 0.754$ without and 0.750 with blade configuration), so the simpler model was retained.

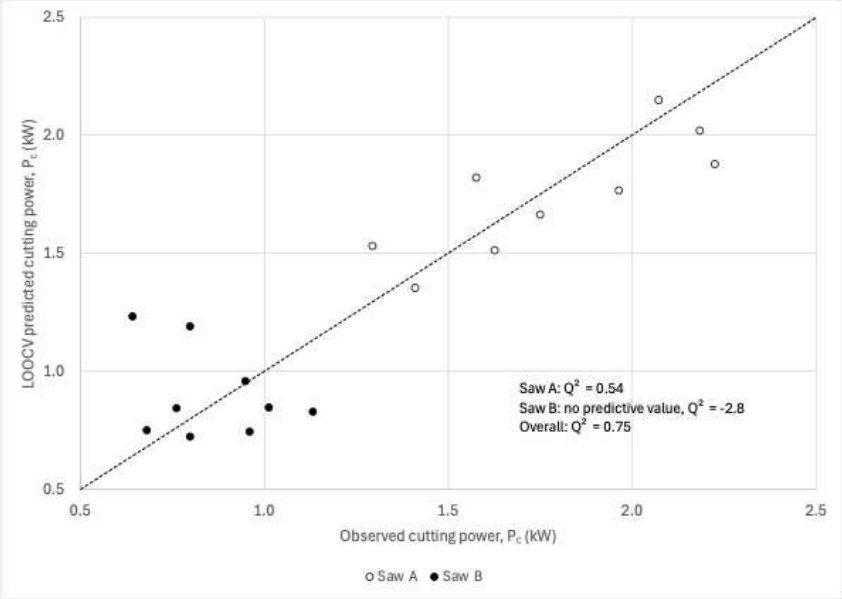


Fig. 8 Leave-one-out cross-validated (LOOCV) predictions of cutting power from the single-predictor model based on mean-square sound pressure (Eq. 3) versus observed values. Open circles: Saw A; filled circles: Saw B. Dashed line: 1:1 line. Within-configuration statistics are computed from the Eq. 3 predictions based on p^2_{rms} (Saw A: $Q^2 = 0.54$, RMSECV = 0.22 kW; Saw B: $r = -0.42$ between predicted and observed values, $Q^2 = -2.8$, RMSECV = 0.30 kW); overall $Q^2 = 0.75$.

Residual diagnostics (Fig. 9, Table 6) showed no significant departure from normality (Shapiro–Wilk $p = 0.30$), no overall heteroscedasticity (Breusch–Pagan $p = 0.97$), and no influential observations (Cook's D max = 0.18) for Eq. 3 (Fig. 9a, b). However, the residuals of Saw B were larger than those of Saw A and decreased with the fitted values, which is consistent with the lack of a within-configuration relationship described above; the two most negative residuals, both from Saw B, lie in the lower tail of the Q–Q plot (Fig. 9b). For Eq. 2, the diagnostics were acceptable (Table 6), although Breusch–Pagan ($p = 0.06$) was borderline and two observations (Saw A, 18 mm) exceeded the 4/n Cook's D threshold; residuals showed no curved pattern once the saw × thickness interaction was included (Fig. 9c, d).

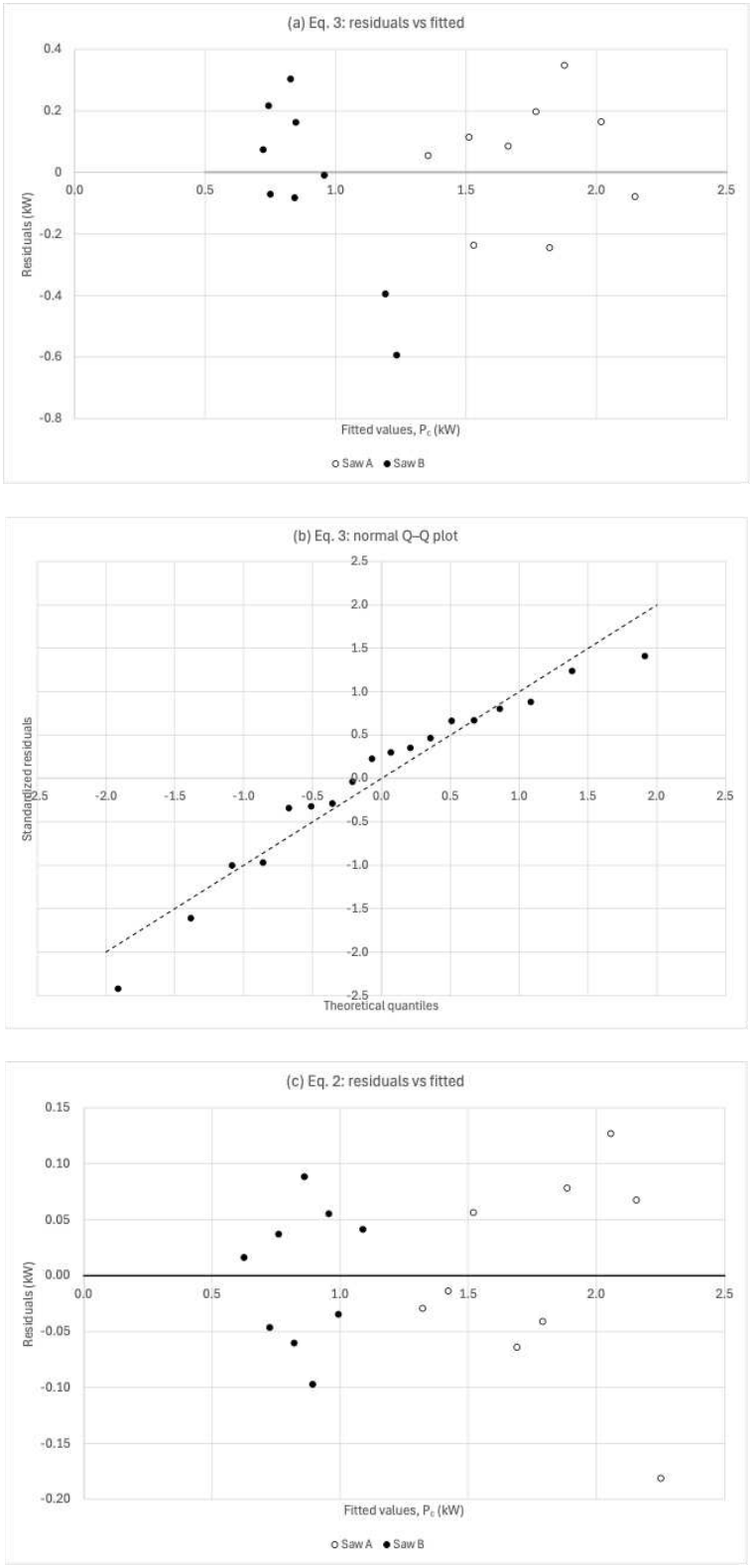
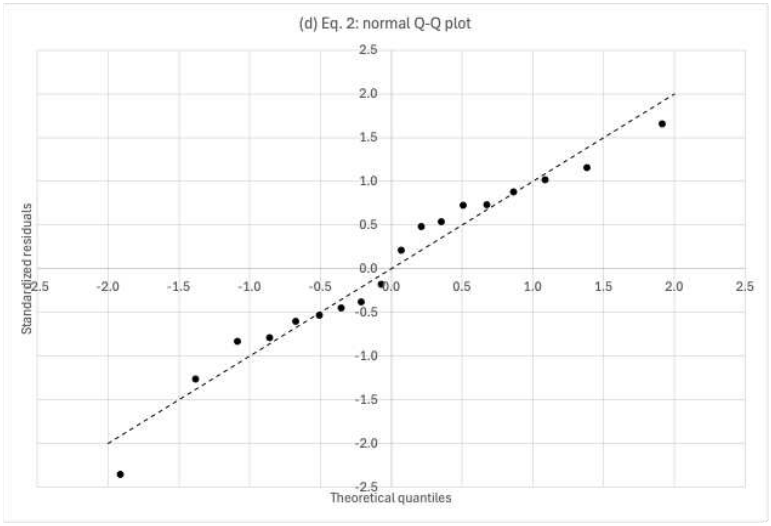


Fig. 9 Residual diagnostics for Eq. 3 (a, b) and Eq. 2 (c–e). (a, c) Residuals versus fitted values; (b, d) normal Q–Q plots of standardized residuals; (e) Cook's D with the 4/n = 0.22 threshold (horizontal line). Open circles: Saw A; filled circles: Saw B (a, c, e).



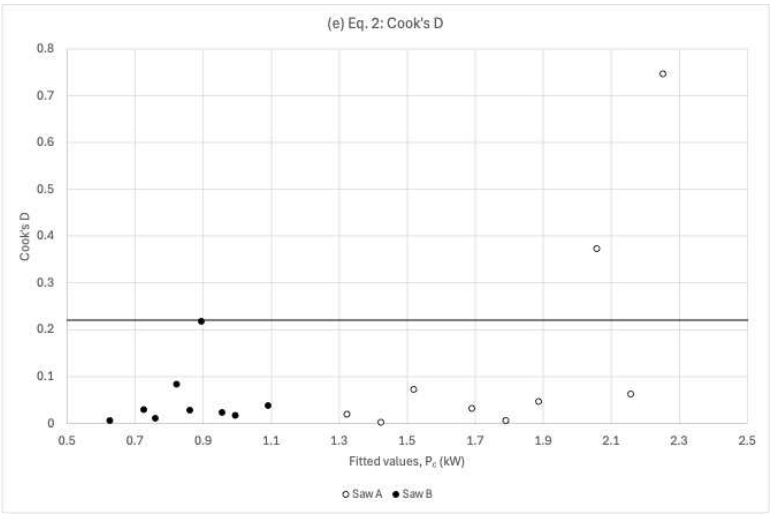


Fig. 9 Cont.

Table 6. Summary of the fitted models and their diagnostics.

Model	Response	Predictors	R^2	RMSECV	Shapiro–Wilk p	Breusch–Pagan p	VIF max	Cook's D max
2	P_c	$I_B + h_c + I_B \cdot h_c + v_f$	0.98	0.11 kW	0.71	0.06	2.0	0.75
—	P_c	MOE	0.01	—	—	—	1.0	—
—	Ra	$I_B + h_c + v_f$	0.12	—	0.53	0.27	1.0	0.25

Model	Response	Predictors	R^2	RMSECV	Shapiro–Wilk p	Breusch–Pagan p	VIF max	Cook's D max
—	Rz	$I_B + h_c + v_f$	0.21	—	0.60	0.13	1.0	0.23
3	P_c	p^2_{rms}	0.80	0.26 kW	0.30	0.97	1.0	0.18

Note: Model 2 is the multiple regression for cutting power (Eq. 2); the Ra and Rz models use blade configuration, panel thickness (continuous), and feed speed, and no term was significant; the MOE-only model is shown to document that it was tested; Model 3 is the simplified model for estimating cutting power from mean-square sound pressure (Eq. 3). VIF for Eq. 2 is reported with h_c centred; without centring it is 39.5 due to the interaction term. For Eq. 2, the maximum Cook's D (0.75) exceeded the conservative 4/n threshold of 0.22 but remained below 1, indicating no observation with strong influence. Two observations (both Saw A, 18 mm) exceeded the 4/n threshold.

This overall performance, however, conceals a marked difference between configurations. The cross-validated error of Eq. 3 was 0.22 kW for Saw A and 0.30 kW for Saw B. For Saw B, this is larger than the standard deviation of cutting power itself (0.16 kW), meaning that the model predicts Saw B no better than its mean. Fitting each configuration separately gave $Q^2 = 0.48$ (Saw A) and -0.41 (Saw B); evaluated within each configuration, the Eq. 3 predictions gave $Q^2 = 0.54$ and -2.8, respectively (Fig. 8). Thus, the apparently good overall prediction is mostly due to the model's ability to distinguish between the two configurations, which differ strongly in both mean-square sound pressure and cutting power, rather than to a sensitivity to variations in power within a configuration.

Mean-square sound pressure can discriminate between the two blade configurations and gives a moderate estimate of cutting power within Saw A, but it did not track cutting power within Saw B, and, pooled across blades, did not respond to panel thickness or feed speed. Whether this behaviour is due to the blade geometry, to the narrower range of power in Saw B (0.49 kW vs. 0.93 kW in Saw A), or to measurement noise cannot be resolved with the present data (n = 9 per configuration). A single-microphone estimator of cutting power would need configuration-specific calibration and evidence that it works for the blade in question; this was not demonstrated for Saw B.

3.4 Sound pressure and surface roughness

Mean-square sound pressure was not related to surface roughness. Across the 18 condition means, the Pearson correlations of p^2_{rms} with Ra and Rz were $r = 0.055$ ($p = 0.83$) and $r = -0.055$ ($p = 0.83$), respectively. Within each blade configuration (n = 9) none of the correlations was significant (Table 7), and their signs differed between blades (positive for Saw A, negative for Saw B), so no consistent trend can be inferred. Spearman rank correlations led to the same conclusion (all $p \geq 0.058$; the closest to significance was Saw B vs Ra, $\rho = -0.65$, $p = 0.058$, with a negative sign). The near-zero overall correlation is consistent with the results of Section 3.2: the two blades differed markedly in p^2_{rms} but not in Ra or Rz. Within Saw B, Ra and Rz tended to increase with mean chip thickness (Section 3.2), whereas p^2_{rms} tended, non-significantly, to decrease with it ($r = -0.52$, $p = 0.15$, $n = 9$), which is consistent with the negative signs of the Saw B correlations in Table 7.

These results differ from the strong sound intensity–roughness correlation reported in routing [9] and from the relationship observed in MDF ripsawing [16]. Acoustic emission has also been analysed in relation to surface roughness in circular saw cutting of beech wood [22]. A plausible explanation is that roughness in plywood is dominated by local features such as veneer tear-out, adhesive layers and

density gradients (Section 3.2), which are not captured by the overall mean-square sound pressure of a cut. In addition, with n = 9 per blade configuration, only correlations with $|r| > 0.67$ would reach significance at $\alpha = 0.05$, so a weak relationship cannot be excluded. Under the conditions tested, mean-square sound pressure did not serve as an indicator of surface roughness.

Table 7. Correlations between mean-square sound pressure and surface roughness.

Group	n	Ra: r (p)	Rz: r (p)
All conditions	18	0.055 (0.83)	−0.055 (0.83)
Saw A	9	0.271 (0.48)	0.168 (0.67)
Saw B	9	−0.484 (0.19)	−0.397 (0.29)

Note: Pearson correlation coefficients (p-values in parentheses) calculated from condition means.

3.5 Limitations

This study has several limitations that should be considered when interpreting the results and their applicability.

First, the experiments were restricted to a single plywood type (radiata pine), with a specific density and moisture content. Other species, veneer qualities, adhesive systems, and MOE values were not evaluated, so the relationships reported here should not be extrapolated beyond this range without further validation. In addition, only one spindle speed (4048 rpm), three panel thicknesses, and three feed speeds were tested, and the sample size was limited to 18 condition means, which reduces the statistical power to detect interactions and increases the risk of overfitting in multi-predictor models. Eq. 2 has five parameters estimated from 18 condition means; although leave-one-out cross-validation supports its predictive performance ($Q^2 = 0.96$, including a nested repetition of the model selection), the specification was data-driven and the ratio of observations to parameters is limited.

Second, because each condition was represented by a single specimen and each panel thickness corresponds to a different plywood panel, the effects of thickness (including the increase of cutting power with thickness, its different slope between blades, and the non-monotonic differences observed in Ra and Rz) cannot be separated from panel-to-panel variability; and because the analyses within each blade configuration rely on only nine condition means, the within-configuration relationships between sound pressure and cutting power (Section 3.3) and between sound pressure and roughness (Section 3.4) are imprecise and should be considered exploratory.

Regarding panel stiffness, MOE varied mainly among specimens within panels (panel thickness accounted for only about 6% of the variance in condition-mean MOE; $F = 0.50$, $p = 0.61$), so the absence of an MOE effect on cutting power is not a consequence of the confounding between thickness and panel. However, MOE spanned a narrow range (condition means 3.58–6.21 GPa), with values above 5 GPa found only in two of the 18 mm conditions, so this result applies only within the range tested.

Third, both saw blades were sharp, and tool wear was deliberately excluded as a variable. Because tool wear is known to affect both cutting power and the acoustic signal, the sound pressure–cutting power relationship may change as the tool wears. Process anomalies (e.g., a dull saw or unexpected material stiffness variations) were not experimentally investigated, and all tests were performed on a single machine and cutting setup.

Fourth, acoustic measurements were taken at a single microphone position (40 cm from the cutting zone, at approximately 45° to the feed direction) in a laboratory environment with a measured background level of 85 dB SPL. The sensitivity of the model to microphone location, source directivity, background noise, and reflections in industrial environments was not evaluated. Only the overall mean-square sound pressure was used; frequency-domain features (e.g., tooth-pass frequency components) were not explored and could provide additional diagnostic information.

Finally, the statistical models are specific to the conditions tested and have not been externally validated. The simplified model for estimating cutting power from sound pressure (Eq. 3) has not been validated in production environments; therefore, its use for real-time monitoring, anomaly detection, or integration into machine control systems should be regarded as a potential future application rather than a demonstrated capability. The within-configuration calibration requirement ($r = 0.81$ for Saw A, no detectable relationship for Saw B) further limits the generality of the approach and should be addressed in future work.

4. Conclusions

This study examined the relationships between cutting power, surface roughness and mean-square sound pressure during radiata pine plywood ripsawing with two circular saw blade configurations. Under the conditions tested, cutting power was associated with blade configuration, panel thickness and feed speed, whereas modulus of elasticity (MOE) did not explain the observed variation within the measured range. Saw B required less cutting power than Saw A within every panel; the apparent increase of this difference with panel thickness cannot be separated from panel-to-panel variability. Because the blades differed in several geometric characteristics, this result applies to the tested configurations and cannot be attributed to tooth count alone.

No meaningful difference in surface roughness was found between the two configurations. Although panel thickness was significant when treated as a categorical factor, its effect cannot be separated from panel-to-panel variability because each thickness was represented by a different plywood panel. The low explanatory power of the roughness models and the high within-condition variability indicate that local material characteristics, including veneer quality and tear-out, may have played an important role.

Mean-square sound pressure clearly distinguished the two blade configurations but was not a universal predictor of cutting power. The strong overall association was largely driven by the separation between the configurations; within-configuration prediction was moderate for Saw A and unsupported for Saw B. Accordingly, the exploratory single-predictor model should not be interpreted as a generally applicable estimator of cutting power. Mean-square sound pressure was not correlated with Ra or Rz, either overall or within either blade configuration, and therefore did not serve as an indicator of surface roughness in this study.

The main limitation is the restricted experimental scope: 18 condition means from one panel per thickness, two sharp blade configurations, one spindle speed and a laboratory acoustic setup. The models have not been externally validated. Further work should include independent panels, additional blade geometries, tool-wear conditions and industrial measurements before sound-pressure-based monitoring of cutting power or surface quality can be recommended.

Authorship contribution

Alfredo Aguilera: conceptualisation, methodology, formal analysis, investigation, writing, reviewing and editing. José Luis Barros: methodology, formal analysis, investigation, reviewing and editing.

Conflict of interest

The authors declare no competing interests.

Data availability

The data that support the findings of this study are available from the corresponding author upon reasonable request.

Acknowledgements

The authors acknowledge the technical support of the personnel of the Forest Products Laboratory at Forest Science and Natural Resources Faculty, as well as the equipment provided by research project Fondecyt 1120347 which was used in the experimental tests and subsequent analysis, and equipment provided by the Acoustic Institute of Engineering Faculty of the Universidad Austral de Chile.

References

1. Klamecki BE (1979) A review of wood cutting tool wear literature. Holz Roh Werkst 37, 265–276. https://doi.org/10.1007/BF02607429

2. Porankiewicz B, Axelsson B, Grönlund A, Marklund B (2011) Main and normal cutting forces by machining wood of Pinus sylvestris. BioRes. 6(4), 3687–3713. https://doi.org/10.15376/biores.6.4.3687-3713

3. Orlowski KA, Ochrymiuk T, Atkins AG, Chuchala D (2013) Application of fracture mechanics for energetic effects predictions while wood sawing. Wood Sci Technol 47, 949–963. https://doi.org/10.1007/s00226-013-0551-x

4. Nasir V, Cool J (2019) Optimal power consumption and surface quality in the circular sawing process of Douglas-fir wood. Eur. J. Wood Prod. 77, 609–617. https://doi.org/10.1007/s00107-019-01412-z

5. Nasir V, Cool J (2021) Cutting power and surface quality in sawing kiln-dried, green, and frozen hem-fir wood. Wood Sci Technol 55, 505–519. https://doi.org/10.1007/s00226-020-01259-1

6. Chuchała D, Orłowski K, Sandak A, Sandak J, Pauliny D, Barański J (2014) The effect of wood provenance and density on cutting forces while sawing Scots pine (*Pinus sylvestris* L.). BioRes. 9(3), 5349–5361. https://doi.org/10.15376/biores.9.3.5349-5361

7. Kminiak R, Gaff M (2015) Roughness of surface created by transversal sawing of spruce, beech, and oak wood. BioRes. 10(2), 2873–2887. https://doi.org/10.15376/biores.10.2.2873-2887

8. Kminiak R, Gašparík M, Kvietková M (2015) The dependence of surface quality on tool wear of circular saw blades during transversal sawing of beech wood. BioRes. 10(4), 7123–7135. https://doi.org/10.15376/biores.10.4.7123-7135

9. Iskra P, Tanaka C (2005) The influence of wood fiber direction, feed rate, and cutting width on sound intensity during routing. Holz Roh Werkst 63, 167–172. https://doi.org/10.1007/s00107-004-0541-7

10. Cyra G, Tanaka C (2000) The effects of wood-fiber directions on acoustic emission in routing. Wood Sci Technol 34, 237–252. https://doi.org/10.1007/s002260000043

11. Iskra P, Tanaka C (2006) A comparison of selected acoustic signal analysis techniques to evaluate wood surface roughness produced during routing. Wood Sci Technol 40, 247–259. https://doi.org/10.1007/s00226-005-0059-0

12. Nasir V, Cool J, Sassani F (2019) Acoustic emission monitoring of sawing process: artificial intelligence approach for optimal sensory feature selection. Int J Adv Manuf Technol 102, 4179–4197. https://doi.org/10.1007/s00170-019-03526-3

13. Nasir V, Kooshkbaghi M, Cool J, Sassani F (2021) Cutting tool temperature monitoring in circular sawing: measurement and multi-sensor feature fusion-based prediction. Int J Adv Manuf Technol 112, 2413–2424. https://doi.org/10.1007/s00170-020-06473-6

14. Chen Y, Tian J, Guo X, Na B (2025) Tool condition monitoring strategies from metal cutting: insights for optimizing wood-based material processing. Eur. J. Wood Prod. 83, 46. https://doi.org/10.1007/s00107-024-02198-5

15. Aguilera A, Martin P (2001) Machining qualification of solid wood of *Fagus sylvatica* L. and *Picea excelsa* L.: Cutting forces, power requirements and surface roughness. Holz Roh Werkst 59, 483–488. https://doi.org/10.1007/s001070100243

16. Aguilera A, Barros JL (2012) Surface roughness assessment on medium density fibreboard rip sawing using acoustic signals. Eur. J. Wood Prod. 70, 369–372. https://doi.org/10.1007/s00107-011-0528-0

17. Nasir V, Ayanleye S, Kazemirad S, Sassani F, Adamopoulos S (2022) Acoustic emission monitoring of wood materials and timber structures: A critical review. Constr Build Mater 350, 128877. https://doi.org/10.1016/j.conbuildmat.2022.128877

18. Juan J (1992) *Comment bien usiner le bois*. Centre Technique du Bois et de l'Ameublement (CTBA), Paris, France. 140 p.

19. Gurău L, Irle M (2017) Surface Roughness Evaluation Methods for Wood Products: a Review. Wood Structure and Function. Curr Forestry Rep 3, 119–131. https://doi.org/10.1007/s40725-017-0053-4

20. Gurău L, Mansfield-Williams H, Irle M (2005) Processing roughness of sanded wood surfaces. Holz Roh Werkst 63, 43–52. https://doi.org/10.1007/s00107-004-0524-8

21. Pinkowski G, Piernik M, Wołpiuk M, Krauss A (2024) Effect of chip thickness and tool wear on surface roughness and cutting power during up-milling wood of different density. BioRes. 19, 9234–9248. https://doi.org/10.15376/biores.19.4.9234-9248

22. Svrzic S, Djurkovic M, Danon G, Furtula M, Stanojevic D (2021) On acoustic emission analysis in circular saw cutting beech wood with respect to power consumption and surface roughness. BioRes. 16(4), 8239–8257. https://doi.org/10.15376/biores.16.4.8239-8257

23. Svrzić S, Djurković M, Vukićević A, Nikolić Z, Mihailović V, Dedić A (2024) Sound classification and power consumption to sound intensity relation as a tool for wood machining monitoring. Eur. J. Wood Prod. 82, 1953–1962. https://doi.org/10.1007/s00107-024-02139-2